stellarator news

Published by Fusion Energy Division, Oak Ridge National Laboratory
Building 5700 P.O. Box 2008 Oak Ridge, TN 37831-6169, USA

Editor: James A. Rome Issue 101 November 2005
E-Mail: jar@ornl.gov Phone (865) 482-5643
On the Web at *http://www.ornl.gov/sci/fed/stelnews*

Sheared plasma flow generation — a new measure for stellarator optimization

Recent stellarator optimization efforts have primarily targeted transport measures such as quasi-symmetry, effective ripple, and alignment of particle guiding center orbits with flux surfaces. For the three forms of quasi-symmetry (helical/toroidal/poloidal), as well as for a variety of nearly omnigenous systems, these efforts have led to significant reductions in neoclassical losses so that, at least for near-term experiments, the neoclassical transport of particles and energy can be made insignificant compared to anomalous transport. However, momentum transport properties provide an additional dimension for characterizing optimized stellarators. The momentum and flow damping features of optimized stellarators can vary widely, depending on their magnetic structure, ranging from systems with near tokamak-like properties in which toroidal flows dominate to those in which poloidal flows dominate and toroidal flows are suppressed. A set of tools [1] has been developed for self-consistently evaluating the flow characteristics of different types of stellarators. Application of this model to existing and planned devices indicates that plasma flow properties vary significantly. Comparisons across devices can aid in unfolding the interplay between anomalous and neoclassical damping effects as well as the impact of momentum transport properties on related plasma phenomena.

Introduction

Plasma flow and momentum transport properties influence a number of important plasma physics issues in stellarators. First, many experiments and simulations have indicated the importance of $\boldsymbol{E} \times \boldsymbol{B}$ velocity shear for turbulence suppression and improved confinement regime access. Reductions in neoclassical viscosity and flow damping can be tied directly to lowered damping of turbulence-driven zonal flows [2]. Generation of sheared flows in stellarators, either through ambipolar electric fields or from external momentum sources such as neutral beams, could be an important hidden variable that should be factored into the international stellarator transport scaling laws. Toroidal flows have been shown [3] to shield resonant magnetic perturbations at rational surfaces, aiding in island suppression. This mechanism may explain the self-healing of flux surfaces often invoked in understanding tokamak discharge evolution. Momentum transport is also

In this issue . . .

a fundamental component in impurity transport analysis [4] and impurity accumulation/shielding studies. Finally, the physics of plasma flow generation and damping in three-dimensional configurations is a productive area for future experiment/theory comparison.

One of the unique aspects of stellarator transport is the fact that radial (perpendicular to flux surfaces) and parallel flows are not coupled as closely as is the case for axisymmetric tokamaks. Although both flows can be expressed in terms of the neoclassical viscous stress tensor [5], the non-ambipolar cross-field flow is typically determined by a projection of the divergence of this tensor in either the toroidal or poloidal direction (depending on which type of quasi-symmetry one is considering). The parallel flows are then derived by inverting the linear system of equations obtained from projecting the divergence of the stress tensor in the magnetic field line direction. As a result, the perpendicular and parallel flows depend on somewhat different weightings of the three stress tensor components. This fact allows stellarators to be designed with similar levels of radial neoclassical transport, but substantially different levels of parallel plasma flow. The parallel plasma flow has a large impact on the net plasma flow patterns within surfaces and on velocity shearing across surfaces. It thus can be an important design variable for optimizing stellarators and a tool for understanding transport differences between existing experiments. In addition, the flows driven by the ambipolar electric field and the structure of the Pfirsch-Schlüter flows (required for incompressibility) must be taken into account in evaluating different stellarator configurations.

Results

In order to demonstrate plasma flow variations among stellarators, a recently developed computational model [1] has been applied to five stellarators (HSX, LHD, W7-X, NCSX, and QPS). This model is based on a moments method approach [6]; for a full description of the model and its applications, see Refs. [1] and [7]. In order to compare these devices on an equal basis, they have been scaled to similar minor radii and magnetic field strengths ($\langle a \rangle = 0.32$, $\langle B \rangle = 1$ T). For simplicity, vacuum equilibria are used, and the toroidal currents are set to zero, except for the case of NCSX, which has about 180 kA of current. The resulting rotational transform profiles of these devices are shown in Fig. 1. The fixed temperature and density profiles shown in Fig. 2 are used for these studies.

In order to explore different collisionality and ambipolar electric field regimes, two parameter sets are considered here: (1) the ECH case, a low-density, $T_e > T_i$ regime [$n(0) = 2.5 \times 10^{19} \mathrm{m}^{-3}$, $T_e(0) = 1.5$ keV, $T_i(0) = 0.2$ keV], and (2) the ICH case, a higher density regime [$n(0) = 8.0 \times 10^{19} \mathrm{m}^{-3}$, $T_e(0) = 0.5$ keV, $T_i(0) = 0.3$ keV].

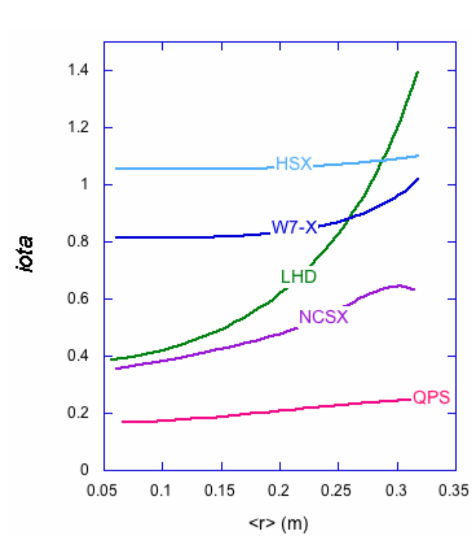

Fig. 1. Rotational transform profiles.

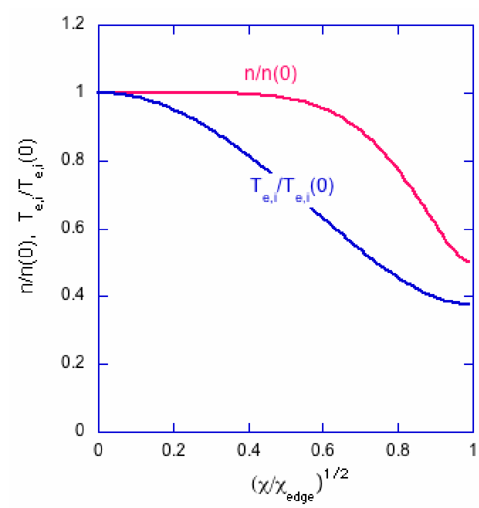

Fig. 2. Density and temperature profiles.

This combination of profiles and parameters has been chosen because they lead to continuously varying ambipolar electric fields (no bifurcations) in each device. Several variations on these profiles, such as increasing central electron temperature in the ECH case, and varying edge pedestal temperatures in the ICH case, can lead to interesting electric field bifurcation phenomena, but these are not pursued here. Also, the generation of poloidal electric fields and their effects on transport are not included in this analysis. The ambipolar electric field profiles obtained from this model for the different devices are shown in Figs. 3 and 4.

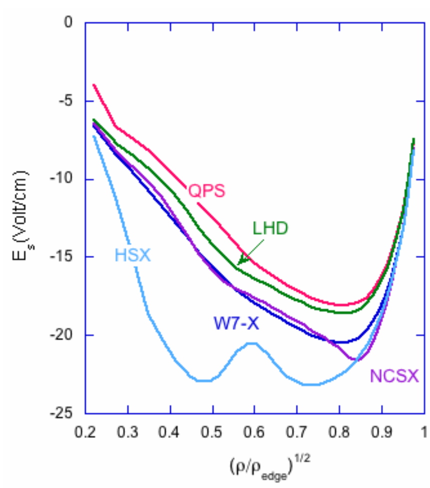

Fig. 3. Electric field profiles for the ICH case.

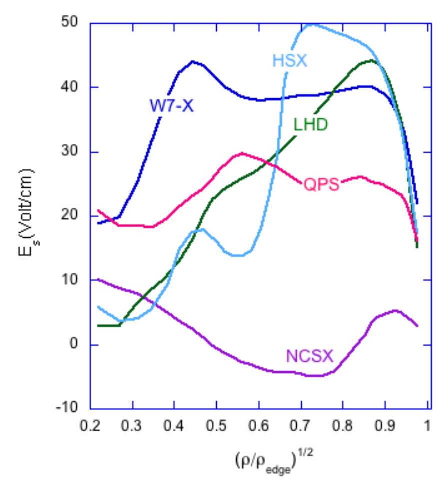

Fig. 4. Electric field profiles for the ECH case.

The ICH parameters lead to inwardly directed electric fields (ion root), while the ECH parameters generally lead to outwardly directed electric fields (electron root). An exception is the NCSX ECH case, which alternates between a positive and a negative electric field (i.e., a Mexican hat profile [8]).

Profiles of the neoclassical parallel ion flow velocity, $v_{||}$, obtained from solving the parallel momentum balance, are presented in Figs. 5 and 6. These and subsequent velocities are plotted in units of meters per second. $U_{||}$ is largest in HSX (due to the high aspect ratio and helical symmetry of this device) and smallest in W7-X (due to bootstrap current suppression optimization and closeness to poloidal symmetry). Parallel flows are small for devices such as QPS and W7-X that are near to poloidal symmetry since the perpendicular diamagnetic and $\boldsymbol{E} \times \boldsymbol{B}$ flows are close to the symmetry direction; the neoclassical viscous stress thus leads only to small parallel flows. This effect is further enhanced in QPS by the low rotational transform. For devices such as LHD, NCSX, and HSX, the perpendicular flows are further from the direction of minimum viscosity and thus must induce larger parallel flows in order for the net flow to minimize the viscous stress. These parallel flows are lower than the sound speed and the ion thermal speed by an order of magnitude or more, justifying the assumption of incompressibility.

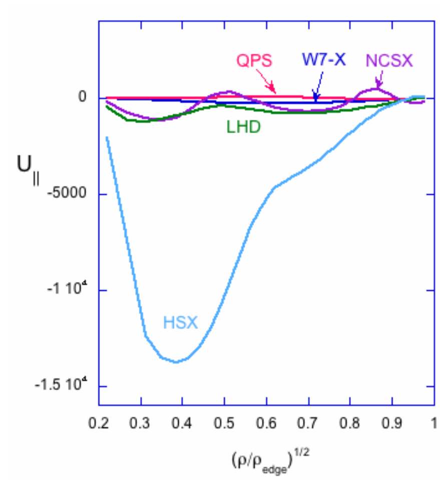

Fig. 5. ICH parallel flow velocity profiles.

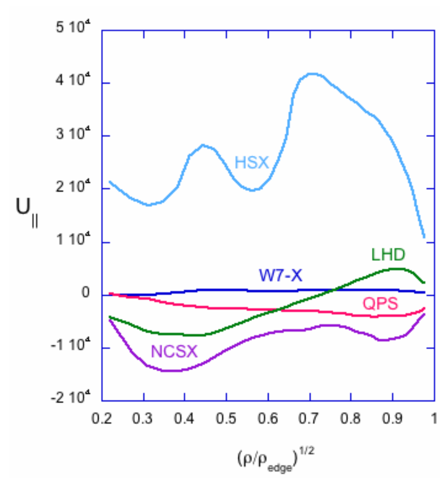

Fig. 6. ECH parallel flow velocity profiles.

Once the parallel flow and Pfirsch-Schlüter flows have been calculated, the poloidal and toroidal components of the total flow (i.e., $\boldsymbol{E} \times \boldsymbol{B}$ + diamagnetic + $U_{||}$ + Pfirsch-Schlüter) can be projected and flux surface averages performed. The specific projections and averaging methods used will depend to some extent on the physics issues to be related to the flow characteristics. Because the connections of two-dimensional flow characteristics to enhanced confinement regimes, island suppression, impurity transport, etc., have not been fully developed for stellarators, a somewhat arbitrary choice has been made for the current study: that is, to project the contravariant components of the flow (in similarity with Ref. [6]), but also to divide by the magnitude of the contravariant basis vectors so that the resulting components have the dimensions of velocity. These components are then flux-surface averaged to give one-dimensional profiles. Two-dimensional flow data on the flux surfaces are also plotted in subsequent figures to provide a more detailed representation. Figures 7 and 8 show the flux-surface averaged poloidal flow components in the different devices for the ICH and ECH cases.

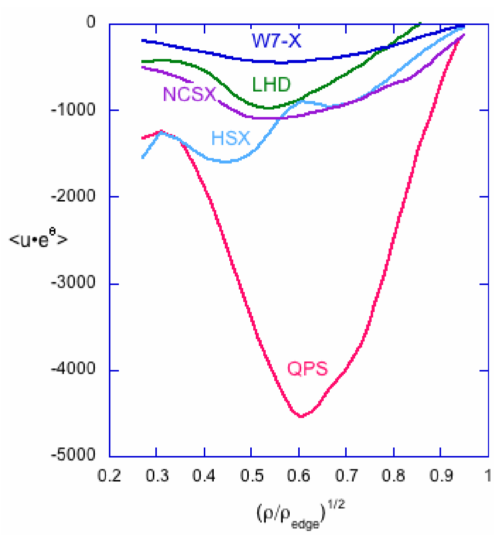

Fig. 7. ICH poloidal flow components.

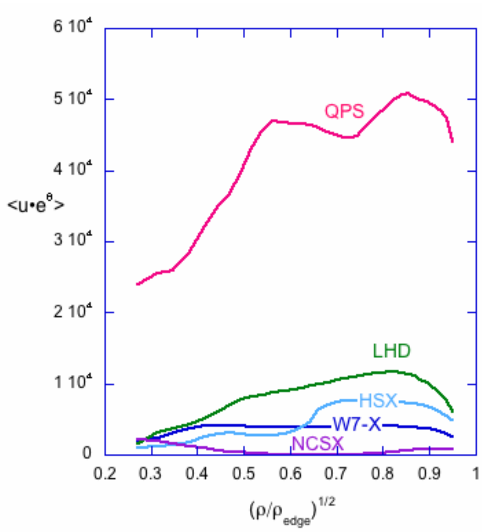

Fig. 8. ECH poloidal flow components.

QPS has very high components of net poloidal flow due to its closeness to quasi-poloidal symmetry. The lowest values of poloidal flow are present in W7-X and NCSX. Similarly, averaged toroidal flow components are plotted in Figs. 9 and 10. In this case, NCSX and HSX have the largest toroidal flows, while QPS, W7-X, and LHD have the smallest components.

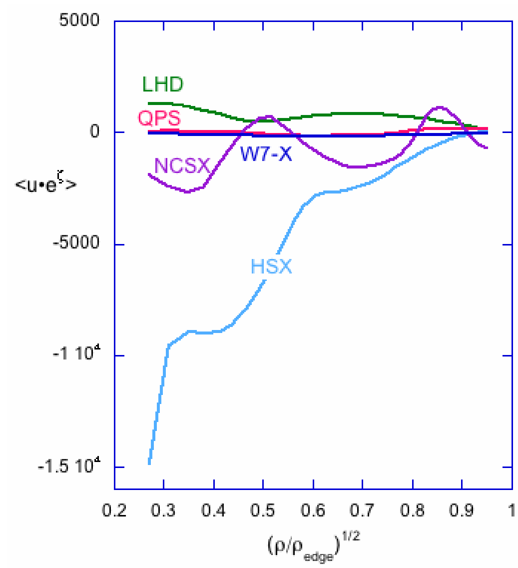

Fig. 9. ICH toroidal flow components.

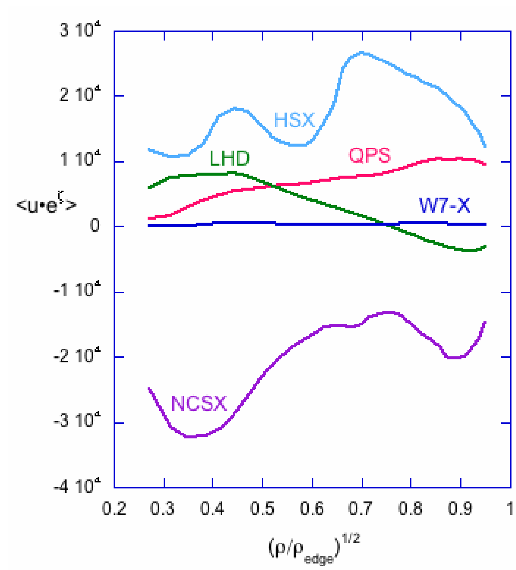

Fig. 10. ECH toroidal flow components.

A primary motivation for the calculation of flow velocities in stellarators is to evaluate the conditions for access to enhanced confinement regimes. Previous simulations and detailed analyses of experiments on tokamaks have highlighted the important role of velocity shearing (in particular, shearing in the $\boldsymbol{E} \times \boldsymbol{B}$ drifts) in suppressing turbulence. In order to evaluate such mechanisms for the configurations analyzed here, the shearing rate for the flux-surface averaged $\boldsymbol{E} \times \boldsymbol{B}$ drift velocity has been calculated. The diamagnetic drift terms are not included because they are already taken into account in the growth rates against which the flow shearing rates are compared. Extensive studies of enhanced confinement regimes in tokamaks [9] have indicated a simple condition for turbulence suppression: the velocity shearing rate should exceed the linear growth rates for modes such as the ion temperature gradient (ITG) mode. The poloidal velocity shearing rates for the five stellarator configurations are compared in Fig. 11 with an estimate from Ref. [9] for the ITG growth rate: ITG = $(C_S/L_T)(L_T/R)^{\mu}$, where L_T is the temperature gradient scale length, C_S is the sound speed, R is the major radius, and μ is a parameter that can vary from 0 to 1. Recently, comparable microinstability growth rates have been evaluated [10] specifically using stellarator equilibria for LHD, W7-X, HSX, QPS, and NCSX. These growth rates range from around $0.2 \times 10^5\ \mathrm{s}^{-1}$ to $1.5 \times 10^5\ \mathrm{s}^{-1}$ for LHD, W7-X, QPS and NCSX and about $4 \times 10^5\ \mathrm{s}^{-1}$ for HSX. This comparison of flux-surface averaged flows effectively assumes that the turbulence is isotropic and uniform over a flux surface, which is not likely to be the case in general, especially for stellarators. Flow shear criteria for nonisotropic turbulence have been discussed in Ref. [11]. The high average poloidal flows of QPS shown in Figs. 7 and 8 are also reflected in high velocity shearing rates that exceed the linear growth rate estimates at the plasma edge. The other configurations approach the lower growth rate estimate ($\mu = 1$) at the edge. These flow shearing rates are based only on the ambient ($\boldsymbol{E} \times \boldsymbol{B}$) flow drives. It is expected that the introduction of external momentum sources, such as neutral beams and RF, will further enhance such shearing rates.

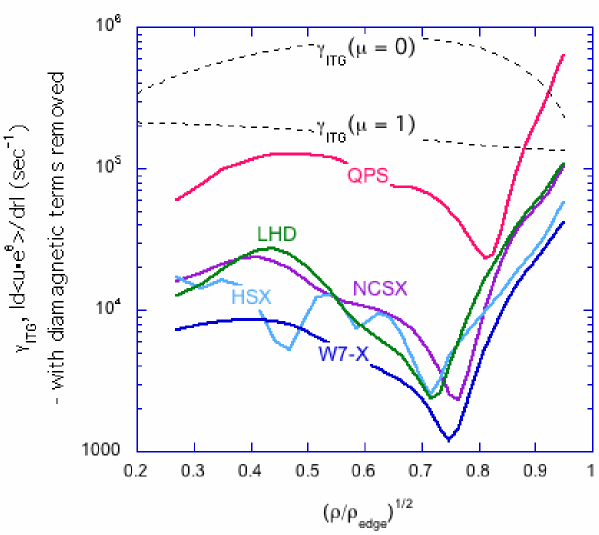

Fig. 11. Radial shearing rate of the ***E*** x ***B*** drift velocity (ICH case) and ITG growth rates.

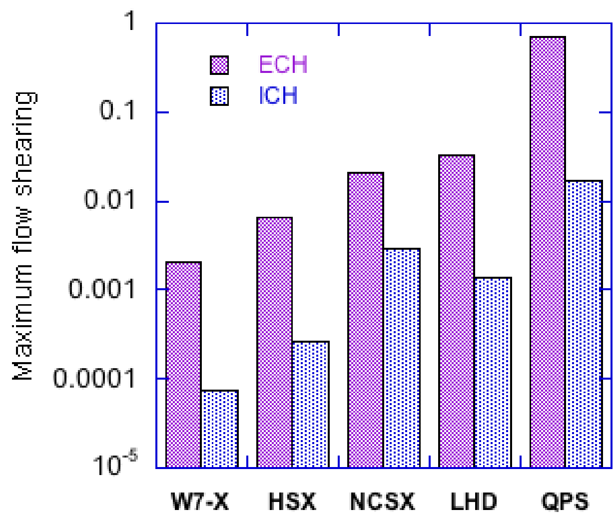

Fig. 12. Maximum parallel shearing rate of the flow velocity normalized to the Alfvén time.

A second measure of velocity shearing to consider in stellarators is the variation of the flow velocity along a field line. This type of shearing would be expected to affect MHD modes, such as ballooning, resistive tearing, etc. The maximum parallel shearing rates within a flux surface at $\chi = 0.75\chi_{edge}$ based on evaluating $\tau_{A0}\left|(\hat{b} \cdot \nabla)\boldsymbol{V}\right|$, where $\tau_{A0} = \langle R \rangle / V_A$ is the Alfvén time, are plotted in Fig. 12 for the two parameter regimes and different configurations. As this shearing rate approaches the level of MHD instability growth rates, some degree of stabilization is expected to occur. The impact of this type of shearing on MHD will depend on whether the MHD mode structure is localized in the same region where the velocity shearing is significant.

In Figures 13–17 the two-dimensional flow variations for ICH parameters on a flux surface at $\chi = 0.75\chi_{edge}$ are displayed. The arrows indicate the direction of flow, and their color is keyed to the local magnitude. These plots are useful in showing details of the flow variations that are lost in the flux-averaged velocity components plotted earlier. Flows in HSX and LHD are predominantly toroidal, indicating that flow velocities are larger where $|\boldsymbol{B}|$ is larger (related to dominance of the parallel flow component). Flows in W7-X begin to show more of a poloidal component and also are generally more uniform in magnitude over the flux surface. This is related to the high aspect ratio and the optimization technique of making the Pfirsch-Schlüter flows close to constant on a flux surface [12]. Flows in NCSX are predominantly toroidal and large in regions where $|\boldsymbol{B}|$ is large; again, this is related to the large parallel neoclassical flow component that is present for quasi-toroidal symmetry. QPS has predominantly poloidal flows that are large in regions where $|\boldsymbol{B}|$ is small. This variation can be related to the very small level of parallel neoclassical flow (which scales as |$\boldsymbol{B}$|) and more dominant $\boldsymbol{E} \times \boldsymbol{B}$ and Pfirsch-Schlüter flows.

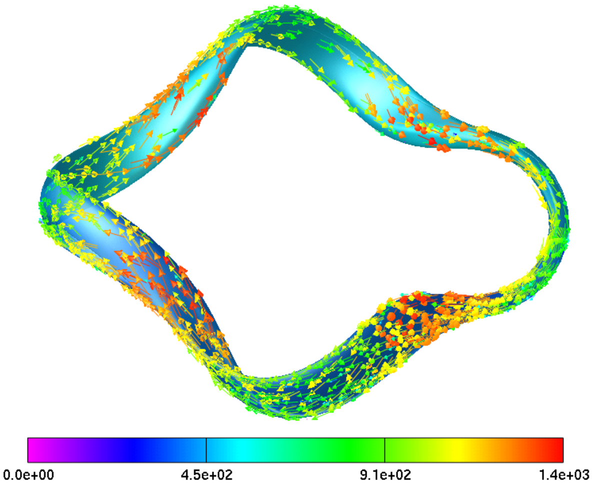

Fig. 13. HSX two-dimensional flow variation.

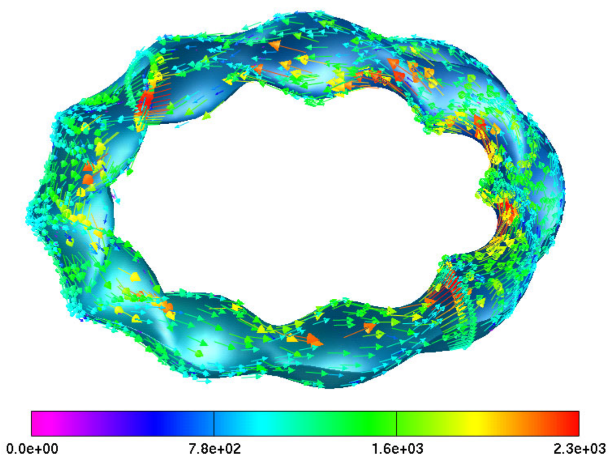

Fig. 14. LHD two-dimensional flow variation.

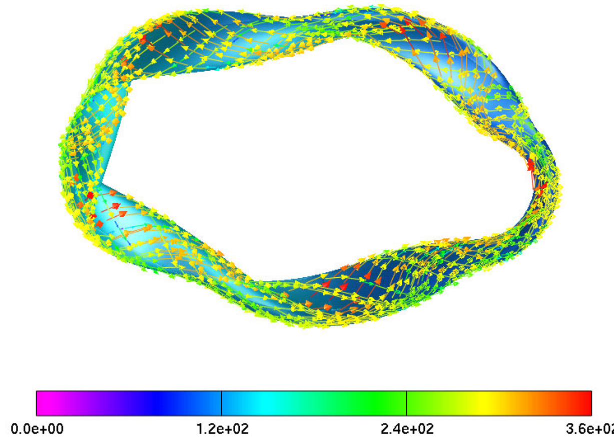

Fig. 15. W7-X two-dimensional flow variation.

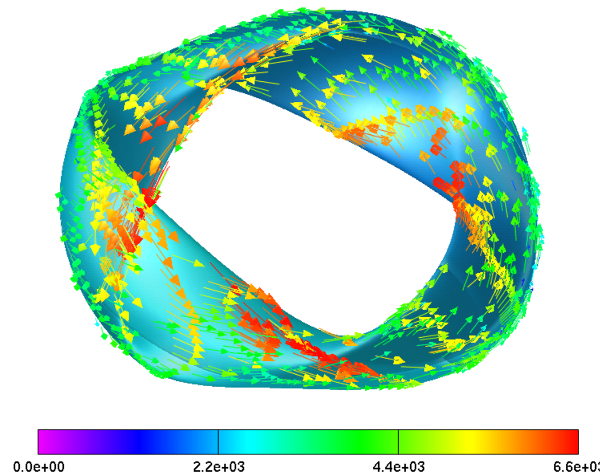

Fig. 16. NCSX two-dimensional flow variation.

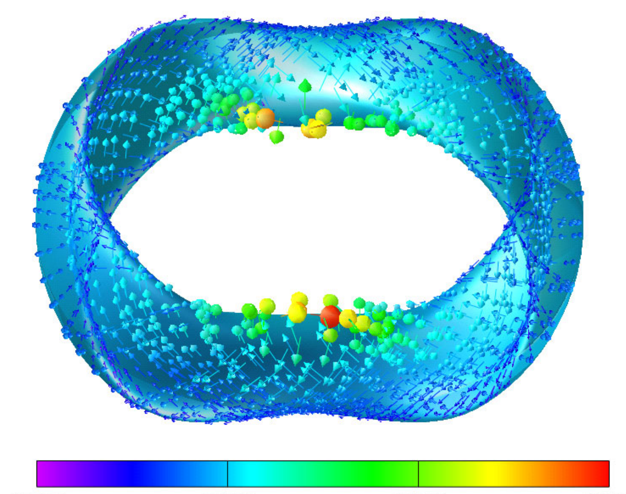

Fig. 17. QPS two-dimensional flow variation.

Conclusions

Differences in plasma flow generation and damping can be observed not only between stellarators and tokamaks, but also among stellarators of different types. Flows in stellarators have two-dimensional variations within magnetic flux surfaces and directional variations ranging from nearly toroidal to nearly poloidal, depending on the dominant magnetic field symmetry. These variations have been demonstrated by applying a moments method model to five different stellarator configurations. In devices such as HSX and NCSX toroidal flows dominate, while in QPS and W7-X poloidal flows dominate. LHD can access both limits, depending on the plasma parameters and profiles used. The variation of flow velocities within flux surfaces reflects the relative magnitudes of the different flow components ($\boldsymbol{E} \times \boldsymbol{B}$ + diamagnetic + neoclassical parallel + Pfirsch-Schlüter). Comparison of poloidal velocity shearing rates with ITG growth rates indicates that in some cases (e.g., the edge region of QPS) shearing rates can exceed ITG growth rates even without the application of external momentum sources, such as beams and RF.

The development of improved methods for calculating the structure of plasma flow velocities in stellarators is intended to stimulate both improved experimental measurements of flows and the development of better theoretical models to assess the impact of these flows on related topics such as turbulence suppression, MHD instabilities, shielding of resonant magnetic field perturbations, and impurity transport. For example, the two-dimensional nature of plasma flows within magnetic surfaces in stellarators will require modeling support for more comprehensive comparisons of theory and experiment. Also, evaluations of turbulence suppression mechanisms and impacts of flows on MHD stability will require extensions beyond simple comparison based on flux-surface-averaged quantities.

The fact that stellarator configurations with similar levels of radial transport can have widely varying flow characteristics (e.g., directionality, variation within a flux surface, shearing rate), coupled with the importance of flow shear to the suppression of anomalous transport, raises the possibility that this can be an important variable both in the optimization of future stellarators and in understanding confinement scaling differences among existing stellarators.

Acknowledgments

Useful discussions with Jeff Harris, Andrew Ware, Steve Hirshman, Hideo Sugama, Shin Nishimura, Wayne Houlberg, Jim Lyon, and Ben Carreras are acknowledged in the development of this model. Research sponsored by the U.S. Department of Energy under Contract DE-AC05-00OR22725 with UT-Battelle, LLC.

Donald A. Spong
Oak Ridge National Laboratory
P.O. Box 2008
Oak Ridge, TN 37831-6169
Phone: (865) 574-1304
E-mail: spongda@ornl.gov

References

[1] D. A. Spong, Phys. Plasmas **12** (2005) 056114.

[2] K. C. Shaing, Phys. Plasmas **12** (2005) 082508.

[3] A. Reiman et al., Nucl. Fusion **45** (2005) 360.

[4] S. Nishimura and H. Sugama, Fusion Sci. Technol. **46** (2004) 77.

[5] K. C. Shaing and J. D. Callen, Phys. Fluids **26** (1983) 3315.

[6] H. Sugama and S. Nishimura, Phys. Plasmas **9** (2002) 4637.

[7] D. A. Spong et al., Nucl. Fusion **45** (2005) 918.

[8] A. Fujisawa, H. Iguchi and T. Minami, Nucl. Fusion **41** (2001) 575.

[9] J. W. Connor et al., Nucl. Fusion **44** (2004) R1.

[10] G. Rewoldt, L.-P. Ku and W. M. Tang, PPPL-4082, June 2005.

[11] T. S. Hahm, Phys. Plasmas **4** (1997) 4074.

[12] G. Grieger et al., Phys. Fluids B **4** (1992) 2081.

15th International Stellarator Workshop

The 15th International Stellarator Workshop (ISW) (October 3–7, Madrid) was a great success. More than 120 experts in stellarator research gathered at CIEMAT and 133 papers were presented. Participants enjoyed fruitful scientific discussions on progress in the last two years and viewed the spectacular phenomenon of an annular eclipse on the first day of the workshop.

In addition to the regular program (4 review talks, 27 invited talks, 12 oral talks, and 89 posters), the program committee arranged a panel discussion on stellarator research in the new era. This panel discussion was designed to stimulate an assessment of stellarator research in light of recent paradigm shifts resulting from the evolution of experimental devices, the rapid growth of stellarator theory, and the impact of ITER and its related broader approach. Although coherent conclusions cannot be well described, a common argument was the need to maximize the competence of stellarators in areas that will not be sufficiently explored even in ITER: steady state, high beta, and plasma-wall interactions. Also the advantages of stellarators, specifically the absence of disruptions and a high density limit, were emphasized.

Indeed, steady extension of operational regimes as regards pulse length and beta has been reported by the Large Helical Device (LHD). Although, unfortunately we must still wait for several years until the next generation of experiments (W7-X, NCSX, QPS) arrives, rapid progress has been made in understanding the effects of helically corrugated magnetic fields experimentally in LHD, TJ-II, Heliotron J, and HSX. In addition, advanced computations aimed at correctly evaluating a figure of merit have suggested the direction of stellarator research. In particular, the feasibility of anomalous transport reduction due to neoclassical transport optimization and the completion of a physics model on stability and beta limits will be primary challenging issues in the coming years.

Materials presented in oral presentations are available on the Web at
http://www-fusion.ciemat.es/SW2005/cover.shtml
thanks to the kindness of the authors. All papers will be available in the proceedings soon, and the program committee has strongly promoted submission of extended papers for publication in a special issue of Fusion Science and Technology.

On this auspicious occasion, the stellarator executive committee expressed gratitude to Prof. Atsuo Iiyoshi for his long years of leadership with a commemorative gift. The next 16th ISW will be in Toki, Japan, in 2007 and will be hosted by the National Institute for Fusion Science.

H. Yamada
Chairman, ISW International Program Committee
E. Ascasibar
Chairman, ISW Local Organizing Committee

Attendees at the 15th International Stellarator Workshop.